Magnetic properties and critical behavior of Fe(tetracyanoethylene)$_2 \cdot x(CH_2Cl_2)$: A high-T_c molecule-based magnet

Mihai A. Gîrţu* and Charles M. Wynn†
Department of Physics, The Ohio State University, Columbus, Ohio 43210-1106

Jie Zhang‡ and Joel S. Miller
Department of Chemistry, University of Utah, Salt Lake City, Utah 84112-0850

Arthur J. Epstein
Department of Physics and Department of Chemistry, The Ohio State University, Columbus, Ohio, 43210-1106
(Received 18 August 1998; revised manuscript received 7 September 1999)

We report magnetic studies of Fe(TCNE)$_2 \cdot x(CH_2Cl_2)$, a member of the family of high-T_c molecule-based magnets, $M(TCNE)_x \cdot y$(solvent) (M=V, Mn, TCNE=tetracyanoethelyne). Based on extensive static and dynamic magnetic measurements we show that this system has a complex magnetic behavior, with a mixture of ferrimagnetic and random anisotropy characteristics. The constricted hysteresis curve with a spin-flop shape, the ac susceptibility in the presence of a dc field, consistent with the spin-flop picture, and the remanent magnetization suggest ferrimagnetic behavior. The ac susceptibility data in zero dc field have modest frequency dependence suggesting glassiness, while the field-cooling/zero-field-cooling magnetization data show irreversibilities, starting at ~97 K, and increasing below ~20 K, all consistent with the behavior of reentrant random anisotropy magnets (RAM). Ferromagneticlike scaling analyses provide a critical temperature T_c =97 K and the critical exponents β=0.45 and δ=2.5, relatively consistent with random anisotropy magnet predictions. Also, the curvature of the $T<T_c$ data in the modified Arrott plot is characteristic for RAM. Correlating the static and dynamic magnetic studies and analyzing the similarities with other members of this family of hybrid organic/inorganic compounds, we discuss the origins of anisotropy and randomness and the possible interconnections between ferrimagnetism and RAM (sperimagnetism) in Fe(TCNE)$_2 \cdot x(CH_2Cl_2)$.

I. INTRODUCTION

The initial discovery of a spontaneous moment at room temperature in the V(TCNE)$_x \cdot y(CH_2Cl_2)$ molecule-based magnet[1] (TCNE=tetracyanoethylene), led to considerable interest in generating a broad class of hybrid organic-inorganic materials[2,3] displaying cooperative magnetic behavior at high temperature. The interest in these unusual systems, for which a substantial fraction of the spin is supplied by p electrons, was stimulated further by the possibility for some of these low-density room-temperature magnets to substitute for ferrites or other materials in various applications.[4]

Earlier magnetic studies of V(TCNE)$_x \cdot y$(solvent) systems (with the solvent being CH_3CN=acetonitrile or C_4H_8O=tetrahydrofuran) revealed[5,6] static critical behavior consistent with existing models for random anisotropy magnets (RAM), previously applied only for site-diluted and amorphous f and d electron systems.[7–11] It also was shown that the spinless organic solvent has a key role in modulating magnetic properties.[5,6]

Using Mn instead of V resulted in the recent synthesis[12] of Mn(TCNE)$_x \cdot y(CH_2Cl_2)$ for which static and dynamic critical analyses revealed[13] reentrant spin-glass behavior, with a high-temperature T transition to a three-dimensional (3D) Heisenberg ferrimagnet and a low T transition to a spin-glass (SG) phase. It was proposed that in that case the random exchange rather than random anisotropy was responsible for the unusual low-temperature behavior.

We report here results of extensive magnetic studies of Fe(TCNE)$_2 \cdot x(CH_2Cl_2)$. Static and dynamic magnetic measurements reveal a rich and complex behavior with both ferrimagnetic and reentrant RAM characteristics. We discuss the possible origins of this unusual behavior based on correlations between static and dynamic magnetic data and, throughout, we compare and contrast the results for Fe(TCNE)$_2 \cdot x(CH_2Cl_2)$ with earlier studies of the other members of the family, mainly V(TCNE)$_x \cdot y$(solvent) and Mn(TCNE)$_x \cdot y(CH_2Cl_2)$.

The outline of this paper is as follows. Section II provides a brief review of RAM theory with an emphasis on some predictions that can be checked experimentally. In Sec. III, we discuss the samples and the experimental techniques, while in Sec. IV we report the results of ac susceptibility and dc magnetization studies, together with static scaling analyses. Section V consists of a discussion of these results in the context of existing models for ferrimagnetism and RAM. Section VI is reserved for conclusions.

II. THEORETICAL AND EXPERIMENTAL BACKGROUND

Theoretical research on magnetic order in disordered systems has concentrated on two different approaches: the first assumes random exchange only, neglecting the effects of random anisotropy leading to the concept of SG,[14,15] while the second assumes that magnetic order is created by random anisotropy in the presence of ferromagnetic exchange, introducing the notion of RAM.[16] The theoretical studies of the RAM were initiated and stimulated by the experimental

work on amorphous alloys of rare-earth and transition-metal ions.[10,17]

Most theoretical studies of RAM are based on the Hamiltonian[16,18,19]

$$\mathcal{H}=-2J\sum_{i,j}\mathbf{S}_i\cdot\mathbf{S}_j-D_r\sum_i(\hat{\mathbf{n}}_i\cdot\mathbf{S}_i)^2-D_c\sum_i(\hat{\mathbf{N}}\cdot\mathbf{S}_i)^2-g\mu_B\sum_i\mathbf{H}\cdot\mathbf{S}_i. \quad (1)$$

The first term is the Heisenberg (ferromagnetic) exchange of strength J ($J>0$), the second is a random uniaxial anisotropy term of strength D_r ($D_r>0$) and local orientation $\hat{\mathbf{n}}_i$, the third is a coherent (nonrandom) uniaxial anisotropy term of strength D_c ($D_c>0$) and orientation $\hat{\mathbf{N}}$, while the last is the Zeeman term due to the applied field $\mathbf{H}$. The continuum version of the RAM Hamiltonian gives the macroscopic energy density:[20]

$$\epsilon=\frac{1}{2}\alpha(\nabla_i M_\mu)(\nabla_i M_\mu)-\frac{1}{2}\beta_r(\mathbf{M}\cdot\hat{\mathbf{n}}_r)^2-\frac{1}{2}\beta_c(\mathbf{M}\cdot\hat{\mathbf{N}})^2-\mathbf{M}\cdot\mathbf{H}, \quad (2)$$

where the magnetization $\mathbf{M}$ is assumed to be of fixed length M_0, $\alpha\propto Ja^2$ (a being an interatomic separation), and β_r and β_c are proportional to the microscopic anisotropies D_r and D_c. In this model the randomness comes from allowing the anisotropy axis $\hat{\mathbf{n}}_r$ to point in arbitrary directions and to change significantly over a spatial scale R_a.

When the random anisotropy is large compared to exchange and the coherent anisotropy is negligible, each spin is directed almost along the random anisotropy axis at its site. Collective behavior is only a secondary phenomenon in this state, called *speromagnetic* (SM).[20,21] When the random anisotropy is weak (and any uniform anisotropy and/or applied field are negligible) the system behaves cooperatively, however, it has no net magnetization.[18,19,22] The local ferromagnetic magnetization changes direction significantly at distances on the order of the finite ferromagnetic correlation length, leading to a correlated spin glass[20] or *correlated speromagnetic* (CSM) state.[10]

In the presence of a moderate applied field a magnetic moment is produced, leading to a field-induced new regime, called the *ferromagnet with wandering axis* (FWA).[20] In the limit of high applied magnetic fields the noncollinear structure aligns even further toward the applied magnetic field, the random anisotropy being able only to slightly tilt the spins from the direction of the applied field. A coherent uniaxial anisotropy can have the effect of an applied field, leading to either one of the states mentioned above, depending on its strength.[20]

These theoretical studies provide important predictions that can be checked experimentally. Discussed below are three such predictions, referring to the field dependence of the magnetization in the approach to saturation, the critical exponents obtained from a ferromagnetic-like scaling analysis, and the curvature of the data in the modified Arrott plots.

The first prediction is for the field dependence of the magnetization for the FWA and the SM. Starting from Eq. (2), Chudnovsky and co-workers introduced[20] the exchange H_{ex}, random anisotropy H_r, and coherent anisotropy H_c fields defined by

$$H_{ex}=\alpha M_0/R_a^2, \quad (3)$$

$$H_r=\beta_r M_0, \quad (4)$$

$$H_c=\beta_c M_0. \quad (5)$$

For the FWA, a RAM with a small random anisotropy ($H_r\ll H_{ex}$) in a moderate applied field ($H_r^4/H_{ex}^3<H<H_{ex}$), it was found that the first-order energy density approach leads, close to saturation, to the following field dependence of the magnetization:[20]

$$\frac{M_0-M(H)}{M_0}=\frac{1}{15}\left(\frac{H_r^4}{H_{ex}^3(H+H_c)}\right)^{1/2}. \quad (6)$$

The same approach gives for the RAM with a small random anisotropy ($H_r\ll H_{ex}$) in the large field ($H_{ex}\ll H$) regime the following expression:[20]

$$\frac{M_0-M(H)}{M_0}=\frac{1}{15}\left(\frac{H_r}{H+H_c+H_{ex}}\right)^2. \quad (7)$$

This last result is valid in the large field limit also for a RAM with large random anisotropy ($H_{ex}\ll H_r$).[20]

Another prediction refers to the critical exponents obtained from a ferromagnetic-like scaling analysis (for systems with the spontaneous magnetization as order parameter). The scaling assumption[23,24] is that near the critical temperature T_c the $M(H,T)$ data obey the scaling equations of state:

$$m^2=\mp a_\pm+b_\pm(h/m), \quad (8)$$

and

$$m=f_\pm(h), \quad (9)$$

where

$$\mathcal{T}=(T-T_c)/T_c, \quad (10)$$

$$m=M/|\mathcal{T}|^\beta, \quad (11)$$

$$h=H/|\mathcal{T}|^{\beta\delta}, \quad (12)$$

and $a_\pm, b_\pm$ are critical amplitudes, while $f_\pm$ are universal scaling functions. The critical exponents β and δ are defined by

$$M\sim|\mathcal{T}|^\beta, \quad (13)$$

valid immediately below T_c in the limit of zero field, and

$$M\sim H^{1/\delta}, \quad (14)$$

valid at T_c. The linear scaling plot [m^2 versus h/m, based on Eq. (8)] and the logarithmic scaling plot [m versus h, based on Eq. (9)] allow the collapse of the magnetization data onto two universal curves, one for $T>T_c$ (+) and one for $T<T_c$ (−). The best such data collapse provides the critical exponents and T_c.

By comparing the equations of state of a RAM and a ferromagnet (FM) Gehring and co-workers[7] were able to predict that for the RAM, the critical exponents (labeled with the subscript a) can be related to the ones of the corresponding FM by[7]

$$\beta_a = \beta \frac{6-d}{2}, \tag{15}$$

$$\delta_a = 1 + \frac{2\gamma}{(6-d)\beta} = \delta - \frac{4-d}{6-d}\frac{\gamma}{\beta}, \tag{16}$$

where d is the lattice dimensionality and $\beta+\gamma=\beta\delta$. Therefore, for meaningful values of d ($d=2$ or 3) $\beta_a > \beta$ and $\delta_a < \delta$. If for a 3D FM system the exponents are $0.32 \leqslant \beta \leqslant 0.36$ and $\delta = 4.87$ (Ref. 23) for the corresponding RAM system they would be $0.48 \leqslant \beta_a \leqslant 0.54$ and $\delta_a = 3.58$.[7]

The modified Arrott plot,[24] is based on the Arrott-Noakes equation of state:[25]

$$(H/M)^{1/\gamma} = a'\mathcal{T} + b'M^{1/\beta}, \tag{17}$$

where a' and b' are critical amplitudes. It allows the determination of the critical parameters by making the $M(H,T)$ data fall on a set of parallel straight-line isotherms (the one at $T=T_c$ passing through origin) by plotting $M^{1/\beta}$ versus $(H/M)^{1/\gamma}$ and choosing appropriately the exponents β and γ. (Note that for the mean-field exponents $\beta=1/2$ and $\gamma=1$ the usual Arrott plot[26] is recovered.)

For RAM the prediction, based on equation-of-state calculations, is that the modified Arrott plots show curves that are not perfectly parallel, especially at low fields, where they curve and shift so that for $T<T_c$ they all pass through the origin[18] or may not intersect the vertical axis at all.[19] This type of low-field behavior reflects the fact that there is no FM long-range order at any finite T (the magnetization goes to zero with the field).

These predictions have been tested experimentally,[10,11] the approach to saturation[5–7,27,28] and the curvature in the Arrott plots being confirmed[5,6,28] while the exponents found are relatively consistent with the expectations.[5–7] Additionally, other types of magnetic behavior may contribute to identifying RAM. The ''rough'' free-energy landscape (with a large number of barriers and valleys with metastable minima) induced by the random anisotropy causes slow relaxation processes and irreversibilities similar to the ones observed in SG.[29,30] Glassy behavior manifested in the frequency dependence of the ac susceptibility and the bifurcation between field-cooled (FC) and zero-field-cooled (ZFC) magnetization have been observed for RAM.[28,31]

III. EXPERIMENTAL

A. Materials

The preparation of $Fe(TCNE)_2 \cdot x(CH_2Cl_2)$ is described elsewhere.[12] This compound has unpaired spins on both the d orbitals of the transition-metal ion and the π^* molecular orbital of the $[TCNE]^-$ bridging organic ion. The results of a Mössbauer spectroscopy study of $Fe(TCNE)_2 \cdot x(CH_2Cl_2)$ confirmed that iron is divalent and high spin ($S=2$).[12] The cyanocarbon acceptor $[TCNE]^-$ has a spin of 1/2 due to an unpaired electron in a molecular orbital of π^* character.

High-spin $3d^6$ Fe^{II} in an octahedral crystal field has a triplet orbital ground state. The orbital momentum is only partially quenched, leading to large deviations of the Landé g factor from the spin-only value.[32,33] Any small distortion from the octahedral symmetry (very common for such systems with triplet ground states) together with the spin-orbit interaction will remove some or all of the orbital degeneracy and introduce magnetic anisotropies with large zero-field splittings,[32,33] which will affect the overall magnetic behavior of the compound.

For $V(TCNE)_x \cdot y(\text{solvent})$ the structural correlation length is short and depends upon the solvent used (e.g., ~10, 15, and 25 Å , when the solvent is CH_3CN, C_4H_8O, and CH_2Cl_2, respectively[5,6]). In contrast, the $Fe(TCNE)_2 \cdot x(CH_2Cl_2)$ diffraction pattern exhibits sharp x-ray diffraction lines similar to the ones observed for $Mn(TCNE)_x \cdot y(CH_2Cl_2)$,[12] indicating a much less disordered partially crystalline structure.

All magnetic data for $Fe(TCNE)_2 \cdot x(CH_2Cl_2)$ were taken on powder samples that were handled in argon and sealed under vaccum in quartz EPR tubes to avoid possible degradation in air. Studies on multiple samples from different batches reproducibly show similar overall behavior. The quantitative variations from sample to sample mentioned throughout the paper are attributed to the differences in solvent content, which was estimated[12] as $0.4 \leqslant x \leqslant 1.1$. For the $Fe(TCNE)_2 \cdot x(CH_2Cl_2)$ reported here, elemental and thermogravimetric analyses lead to an estimation of $x \sim 0.72$.

B. Experimental techniques

The measurements of the linear ac magnetic susceptibility and its harmonics were made with a Lake Shore 7225 ac Susceptometer/dc Magnetometer first in zero applied dc field in the temperature range $5 \leqslant T \leqslant 150$ K, on warming. Both the in-phase (χ') and out-of-phase (χ'') linear susceptibilities, $\chi = \chi' + i\chi''$, were measured under an ac field $H_{ac} = H_0 \sin(2\pi ft)$ with $H_0 = 1$ Oe and a wide range of frequencies f ($5 \leqslant f \leqslant 10\,000$ Hz). Measurements of the linear ac magnetic susceptibility as a function of applied dc fields $0 \leqslant H \leqslant 50\,000$ Oe were made at constant T, in the temperature range $5 \leqslant T \leqslant 100$ K, with $H_0 = 1$ Oe and $f = 1$ kHz, after the zero dc field measurements.

The dc magnetization was measured with a Quantum Design MPMS 5 magnetometer. The temperature dependence of the static susceptibility was determined based on magnetization data collected on cooling between 350 and 5 K in a dc applied field of 5000 Oe. Hysteresis curves were obtained at 5 K for applied fields of $-55\,000 \leqslant H \leqslant 55\,000$ Oe, after cooling with no applied field through the transition. The remanent magnetization was measured after taking precautions for properly zeroing the applied dc field, to within 0.05 Oe. The sequence for the measurements consisted of cooling the system in a small dc field (10 Oe at first) from 150 to 5 K, well below the transition; turning the applied field to zero at 5 K; taking data on warming in zero applied dc field at ~0.2 K/min; repeating the sequence for higher fields, up to 50 Oe. (Fields higher than 50 Oe were avoided because of the danger of trapping flux in the superconducting magnet which would than compromise the zeroing of the dc field. Fields lower than 10 Oe lead to noisy data.)

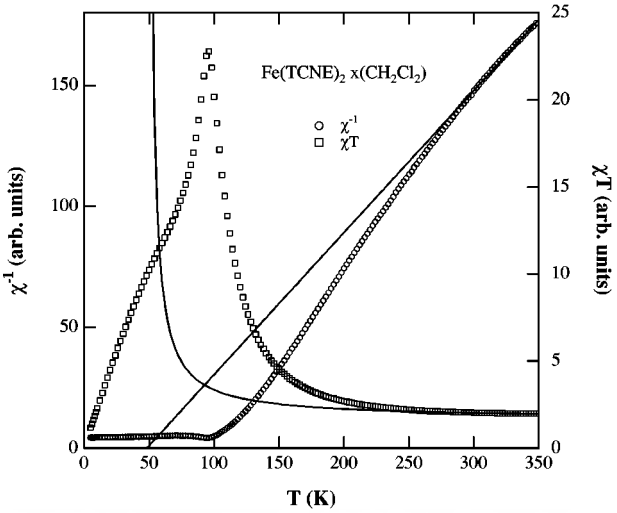

FIG. 1. χ^{-1} as a function of T (left axis) and χT as a function of T (right axis), measured in dc applied fields of 5000 Oe. The solid lines are a fit to the Curie-Weiss mean-field law in the range $250 \leqslant T \leqslant 350$ K.

Field-cooled (FC) and zero-field-cooled (ZFC) magnetization data were collected on warming in the range $5 \leqslant T \leqslant 150$ K in various applied dc fields. The sequence for the measurements consisted of cooling the system in zero applied dc field from 150 K to 5 K; turning the applied field on at 5 K; taking ZFC data on warming at ~0.5 K/min in the applied dc field; cooling the system in the same applied dc field from 50 K to 5 K; taking FC data on warming in the applied dc field; repeating the sequence for higher fields ($10 \leqslant H \leqslant 500$ Oe).

IV. RESULTS AND ANALYSIS

The dc susceptibility $\chi(=M/H)$ in the range 5–350 K at $H=5000$ Oe is displayed as χ^{-1} and χT versus T in Fig. 1. The χT product increases as T is lowered from 350 K, with a peak near 97 K. A simple fit of the χ data to the mean-field Curie-Weiss law $\chi = C/(T-\theta)$ (shown as solid lines for both χ^{-1} and χT in Fig. 1 for $250 \leqslant T \leqslant 350$ K gives a value of $\theta = 50$ K. The range of temperature $250 \leqslant T \leqslant 350$ K for a good fit suggests that probing the dc susceptibility at higher T would be necessary to reach the true Curie-Weiss regime.

While the temperature of the peak in the dc susceptibility is consistently the same from batch to batch, the magnitude may vary by as much as 50%. Correspondingly, while θ is nearly the same, the value of the Curie constant C varies from batch to batch, likely due to the differences caused by the solvent content.[34] Due to the variation in C and unknown Landé g factor the number of spins cannot be precisely determined.

The in-phase χ' and out-of-phase χ'' components of the complex ac susceptibility as a function of T, at various frequencies, in the absence of an applied dc field are shown in Fig. 2. The real part of the susceptibility displays a clear peak at ~97 K and a broader feature at ~25 K, while χ'' has a weak peak at ~97 K and a stronger one below 20 K. As the imaginary part of the susceptibility is related to losses, the weak peak at high T suggests a transition with small hysteresis. The frequency dependence of χ' is weak, starting

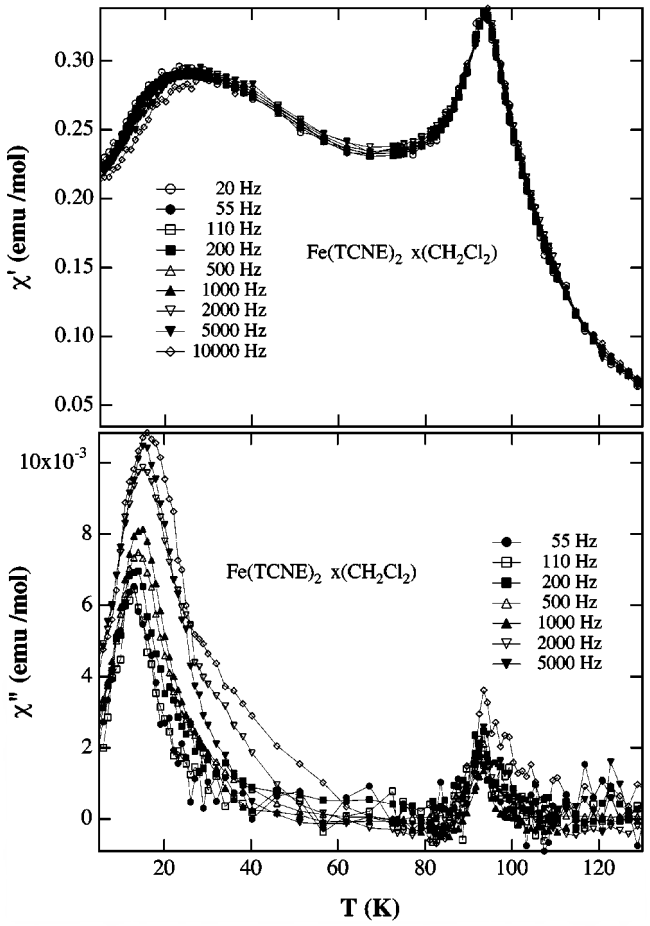

FIG. 2. χ' and χ'' as funtions of T, measured at $H=0$, $H_0=1$ Oe, and $20 \leqslant f \leqslant 10\,000$ Hz. The χ'' 20 and 10 000 Hz data were too noisy to be shown.

below 90 K and becoming more obvious only below 40 K. Despite being noisy, especially at low frequencies, the χ'' data show a much clearer frequency dependence at and below 20 K.

ZFC and FC magnetizations, Fig. 3, were measured in

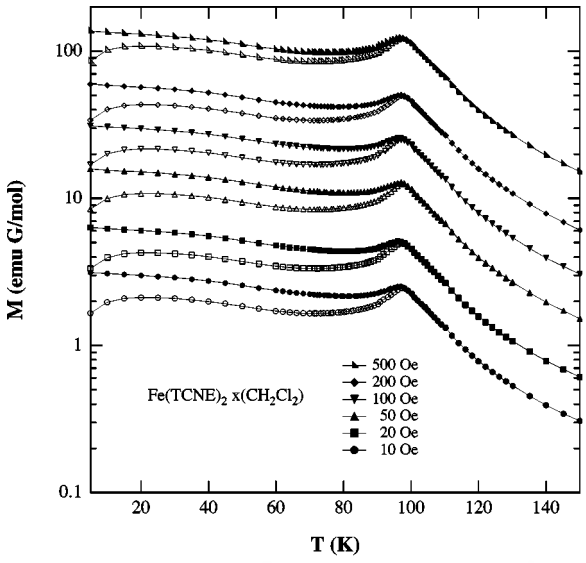

FIG. 3. FC (filled symbols) and ZFC (empty symbols) magnetizations as functions of T for $10 \leqslant H \leqslant 500$ Oe.

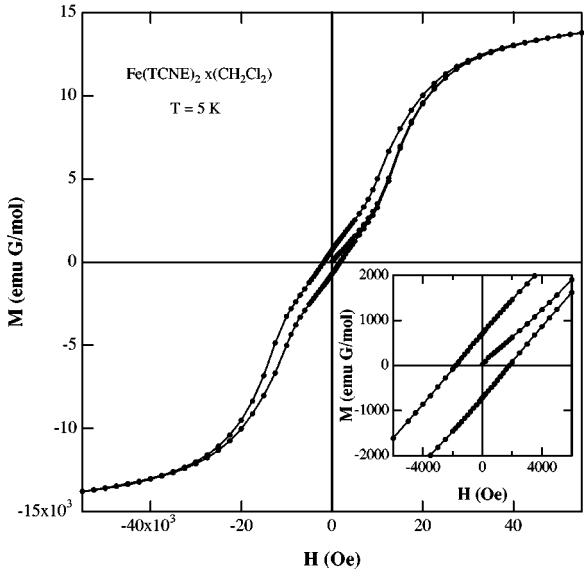

FIG. 4. $M(H)$ hysteresis curves [including the initial ZFC $M(H)$ curve starting at origin] at 5 K, for dc fields up to 55 kOe. The inset shows a detail of the low-field region with small remanence and a coercive field of ~2000 Oe.

various applied dc fields ($5 \leqslant H \leqslant 500$ Oe), on warming. Irreversibilities manifested as $M_{FC} \neq M_{ZFC}$ start at the bifurcation point observed near ~97 K and become more pronounced below ~20 K.

The hysteresis curve taken at 5 K, Fig. 4, has an unusual constricted shape with an inflection point at $\sim \pm 10$ kOe reminescent of spin-flop field-induced transitions.[35] The inset of Fig. 4 shows a low-field detail of the hysteresis loop with small remanence and a coercive field of ~2000 Oe. It is noted that while the shape and the position of the inflection point is the same from batch to batch differences in the magnitude of the saturation magnetization arise, likely from the variance in solvent content.[34]

Results of dynamic susceptibility measurements in the presence of an additional applied dc magnetic field are shown in Fig. 5. At high T (above the transition) χ' decreases monotonically with increasing dc field. As the temperature is lowered, a peak in χ' is observed down to 5 K. The peak position shifts systematically toward higher applied fields, moving from ~8 kOe at 90 K to ~13 kOe at 5 K. The magnitude of the peak in χ' has a maximum at ~70 K and decreases again upon lowering T. The existence of a peak in $\chi'(H)$ indicates a maximum in dM/dH, which can be related to a metamagnetic or a spin-flop transition, consistent with the hysteresis data.

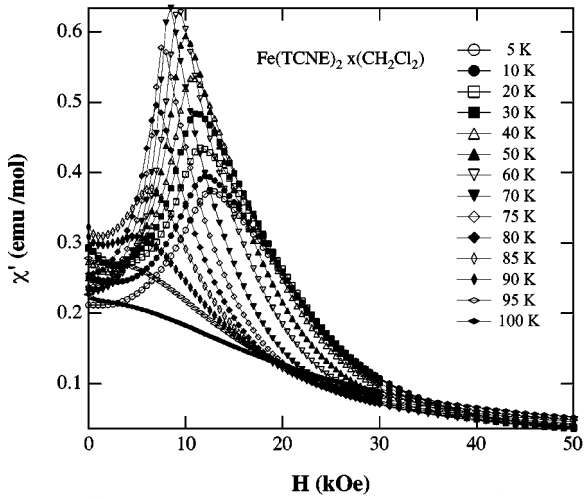

FIG. 5. χ' as a function of H, measured at $H_0 = 1$ Oe and $f = 1000$ Hz, in the range of $5 \leqslant T \leqslant 100$ K.

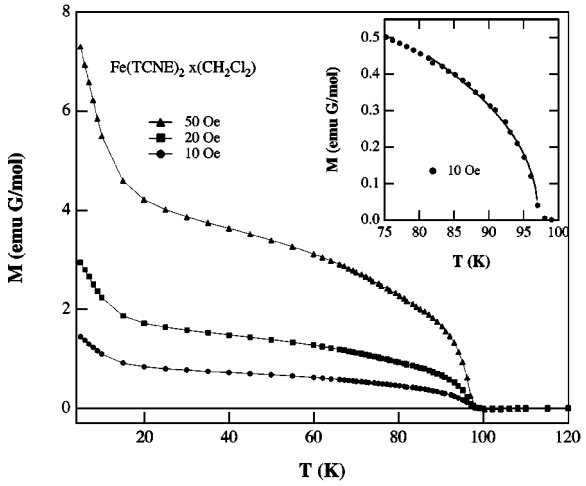

FIG. 6. Remanent magnetization as a function of T, measuring after cooling in dc fields of 10, 20, and 50 Oe. The inset shows a detail of the 10 Oe data with the critical region and the power-law fit (solid line) based on Eq. (13). The values obtained from the fit are $T_c = 97.05$ K and $\beta = 0.45$, for $0.002 \leqslant T \leqslant 0.18$.

Remanent magnetization M_{rem} was measured on warming in zero field after cooling in various dc fields, to probe the formation of a spontaneous moment. The remanent magnetization, Fig. 6, drops sharply with increasing T from 5 to 20 K, decreases gradually up to 90 K and vanishes abruptly at ~97 K. The shape of the curve is independent of H.

To further probe the high-T transition we attempted a static ferromagneticlike critical analysis. To determine the critical parameters separately we used first the remanent magnetization data to get initial estimates for T_c and β based on Eq. (13), and then the critical isotherm to determine δ based on Eq. (14).[36]

The fit of the low-field remanent magnetization (assuming that it is the best probe of the spontaneous magnetization) to the power-law behavior below T_c, according to Eq. (13) (inset of Fig. 6), for a range of the reduced temperature of $0.001 \leqslant T \leqslant 0.2$, gives $T_c = 97.05$ K and $\beta = 0.45$. The errors in the determination of these values are estimated to below $\pm 2\%$ for T_c and about $\pm 5\%$ for β, mainly due to the various possible choices for the temperature ranges where the data were fitted. The final choices were made such that the region fitted was within the expected critical regime, and such that the best fit could be obtained. We note that fits of the higher field data gave similar T_c's but systematically lower values for β (96.98 K and 0.42, for 20 Oe; 96.93 K and 0.40, for 50 Oe).

Isothermal magnetization data $M(H)$, Fig. 7, were collected for various T (74–118 K, starting with the highest T) by zero-field cooling and measuring from 0 to 55 kOe, to perform a static critical analysis near the transition. M increases monotonically with decreasing T. At the low limit of

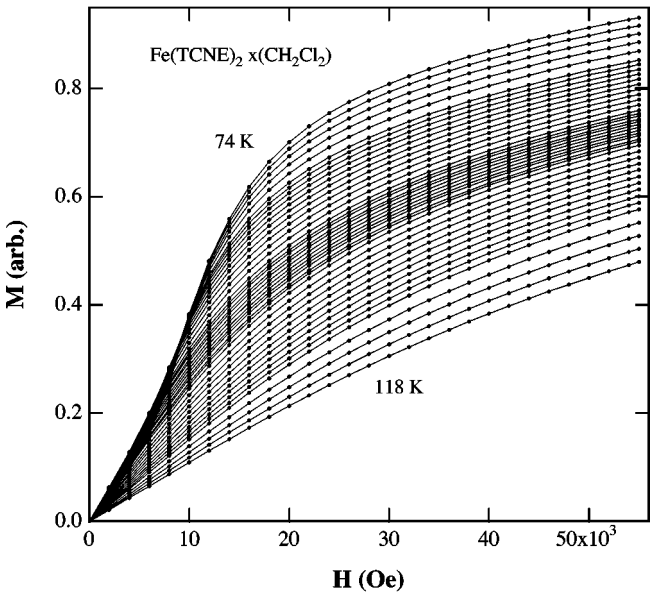

FIG. 7. $M(H)$ as measured at various T ranging from 74 to 118 K. Data was collected every 2 K in the range 74–84 K and 110–118 K, every 1 K for 84–90 K and 104–110 K, every 0.5 K for 90–94 K and 100–104 K, every 0.2 K for 94–96 K and 98–100 K, every 0.1 K for 96–98 K. For clarity, only data for selected temperatures (every 2 K in the range 74–84 K and 110–118 K, every 1 K for 84–94 K and 100–110 K, every ~0.5 K for 94–100 K) are shown.

the temperatures scanned $M(H)$ has the S shape seen in the 5 K hysteresis curve (Fig. 4), consistent with the results for the ac susceptibility in a dc superimposed field (Fig. 5).

Choosing $T=97.0$ K, obtained from the scaling analysis of the remanent magnetization, as the initial estimate for T_c, the fit based on Eq. (14) of the magnetization on the critical isotherm gives $\delta=2.77$, Fig. 8. The error of this value is estimated to $\sim\pm 10\%$, again due to the various possible H ranges for fit. The criterion has been to choose values of H

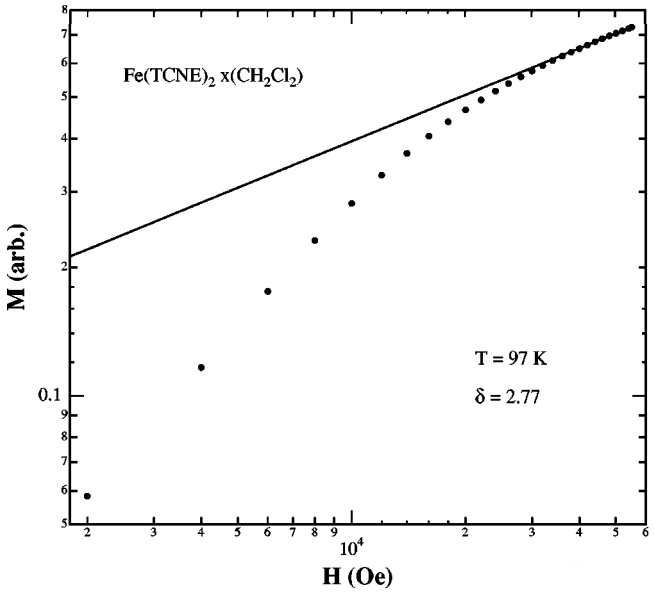

FIG. 8. $M(H)$ isotherm at 97 K with a fit (solid line) to a power law in H based on Eq. (14). The critical exponent obtained from fitting in the range $30\leq H\leq 55$ kOe is $\delta=2.77$.

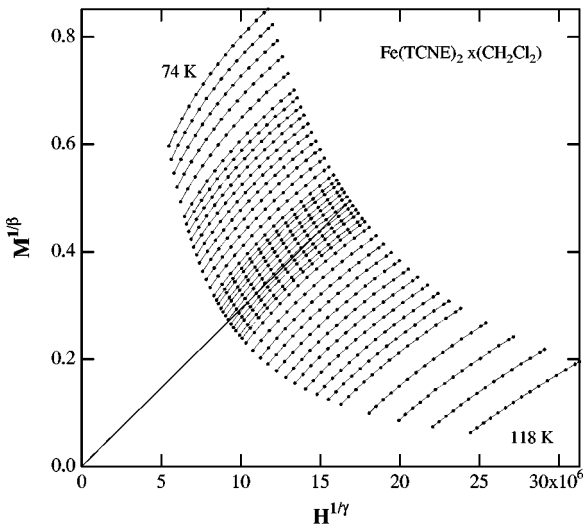

FIG. 9. Modified Arrott plots [$M^{1/\beta}$ versus $(H/M)^{1/\gamma}$] of the $H\geq 2$ T $M(H)$ data from Fig. 7 for $\beta=0.45$ and $\delta=2.5$. For clarity, only data for selected temperatures (see Fig. 7) are shown.

that are large enough to remove possible domain-wall effects but small enough compared to T_c ($\mu_B H\ll k_B T_c$).[24]

The values for β and δ obtained as described above were used as initial guesses to obtain the modified Arrott plots[24] $M^{1/\beta}$ versus $(H/M)^{1/\gamma}$ displayed in Fig. 9. The modified Arrott curves in Fig. 9 preserve some curvature even in the vicinity of the transition for every choice of critical exponents, which made more difficult the determination of the critical exponents. Therefore, the operational criterion for the choice of critical exponents based on Arrott plots is to obtain parallel curves over as wide range as possible, particularly in the high-field regions.[37]

The final choice of the scaling parameters was made judging by three simultaneous criteria, which in order of their importance were best data collapse on the linear scaling plot (Fig. 10), best data collapse on the logarithmic scaling plot (Fig. 11), and largest range of parallel curves in the modified Arrott plot (Fig. 9). The linear scaling plot, Fig. 10, and the logarithmic scaling plot, Fig. 11, allowed the collapse of the magnetization data on the two universal curves. The linear plot was found to be more sensitive to the choice of the critical exponents, as the logarithmic scales tend to hide departures from data collapse.[24] The scaling parameters that met the three criteria mentioned above were $T_c=97$ K (with an estimated error of below $\pm 2\%$), $\beta=0.45$ ($\pm 5\%$) and $\delta=2.5$ ($\pm 10\%$), while the range of reduced temperatures was $0.001\leq|\mathcal{T}|\leq 0.23$.

V. DISCUSSION

In this section we discuss the data and the results of the analysis for $Fe(TCNE)_2\cdot x(CH_2Cl_2)$ in the context of ferrimagnetism, RAM, and reentrance. Throughout, we compare and contrast the results reported here with earlier studies of the other members of the family, mainly $V(TCNE)_x\cdot y(\text{solvent})$ and $Mn(TCNE)_x\cdot y(CH_2Cl_2)$.

A. Ferrimagnetic behavior

The Curie-Weiss fit of the dc susceptibility data (Fig. 1) gives a positive θ due to the limited range of temperatures

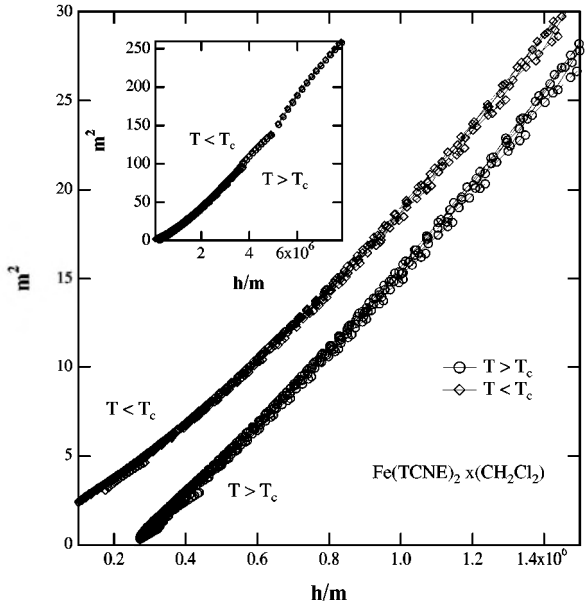

FIG. 10. Static scaling analysis on a linear plot of $m^2 = (M/|T|^{\beta})^2$ versus $h/m = H/(M|T|^{\gamma})$ using $H \geq 2$ T $M(H)$ data. Data collapse is obtained for $T_c = 97$ K, $\beta = 0.45$, and $\delta = 2.5$. Inset shows entire range of data.

available. Higher T data may lead to negative θ, which would indicate ferrimagnetic behavior. A similar behavior was seen in the related compound $Mn(TCNE)_x \cdot y(CH_2Cl_2)$,[13] in which case, based on data available from other Mn-based compounds bridged by TCNE,[3,38] an antiferromagnetic coupling between the $S = 5/2$ Mn^{II} and the spin 1/2 $[TCNE]^-$ was proposed. In the case of $Fe(TCNE)_2 \cdot x(CH_2Cl_2)$ a similar antiferromagnetic coupling between the $S = 2$ Fe^{II} and the spin 1/2 $[TCNE]^-$ is expected due to superexchange (virtual reverse electron transfer from $TCNE^-$ to Fe^{II}).

The hysteresis curves (Fig. 4) are constricted with a spin-flop shape, consistent with the ac susceptibility data taken in a dc field (Fig. 5). For the field-induced transition to take place an H of about 10 kOe is needed. This behavior is

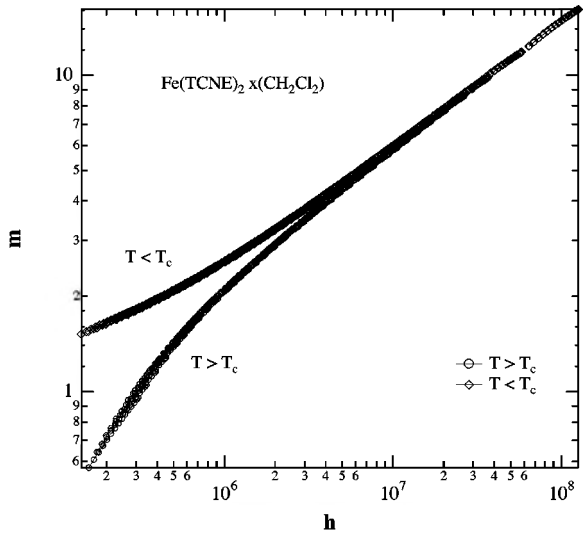

FIG. 11. Static scaling analysis on a log-log plot of $m = M/|T|^{\beta}$ versus $h = H/|T|^{\beta\delta}$ using $H \geq 2$ T $M(H)$ data. Data collapse is obtained for $T_c = 97$ K, $\beta = 0.45$, and $\delta = 2.5$.

consistent with the antiferromagnetic coupling between the spins on the transition-metal ion and the ones on the organic ligand, and with the existence of sublattices, the spins of which can flip due to the applied field.

Also, the remanent magnetization (Fig. 6) has an unusual shape. Such shapes were observed previously in the similar compound $Mn(TCNE)_x \cdot y(CH_2Cl_2)$,[13] as well as in various ferrites[39] and were accounted for based on the existence (at least locally) of different sublattices, within the ferrimagnetic system, each with its own temperature dependence of the sublattice magnetization.

B. Double-transition RAM behavior

The ac susceptibility data in zero dc field (Fig. 2) has some frequency dependence (better seen in χ'') enhanced below ~20 K consistent with reentrant SG's (Refs. 29,30) or double transition RAM's (Ref. 10) but not with regular ferromagnets or ferrimagnets. Irreversibilities, starting at ~97 K and increasing below ~20 K, are observed in the FC/ZFC magnetization data (Fig. 3). Such behavior suggests slow relaxation processes usually present in reentrant random exchange[29,30] or double-transition random anisotropy systems.[10] However, that the remanent magnetization is different from zero, suggesting that there is a spontaneous magnetization in the system below the 97 K transition, demonstrates that this system is not a typical SG.[29,30]

The deviations from parallelism in the modified Arrott plots (Fig. 9) also suggest that this system is neither a typical FM nor a typical ferrimagnet. Moreover, ferromagneticlike scaling analyses showed through the successful data collapse that the magnetization is a valid order parameter and, consequently, this system cannot be a SG. Furthermore, the values obtained for the critical exponents are out of the range of typical crystalline[23,24] or amorphous[43] ferromagnets,[23] but relatively similar to the ones obtained for RAM's.[7,42,44] Also, in the case of $Fe(TCNE)_2 \cdot x(CH_2Cl_2)$ for $T < T_c$ the modified Arrott plot curves (Fig. 9) are concave, bending toward the horizontal axis as expected for RAM's.[18,19,28]

For RAM a double transition was observed in rare-earth alloys.[45,46,27] The theoretical explanation proposed was[20] that temperature-dependent anisotropy causes a low temperature crossover from a CSM to a SM (the high-T transition being from a paramagnet to a CSM). Hence, an increased low-T random anisotropy causes the system to ''freeze'' even further and appear more disordered, spin glasslike.

To explore the nature of the low-T state of the system we compared in Fig. 12 the low-temperature magnetization data (the virgin curve in the hysteresis plot of Fig. 4) with the predictions of Eqs. (6) and (7). Equation (6) is valid for a FWA, a RAM with small anisotropy in a moderate applied field ($H_r^4/H_{ex}^3 < H < H_{ex}$), while Eq. (7) is valid for a RAM with small anisotropy at high fields ($H_r^4/H_{ex}^3 < H_{ex} < H$) and also for a RAM with high anisotropy at high fields ($H_{ex} < H_r < H$). The fit was performed in a limited range of dc fields ($30 \leq H \leq 55$ kOe), close to saturation, to avoid the region with spin-flop behavior at ~13 kOe. The results for the moderate field approximation were $M_0 \approx 19\,100$ emu Oe/mol, $H_r^4/H_{ex}^3 \approx 920$ kOe, and $H_c \approx 0.1$ Oe, while the quality of the fit was relatively poor. In the large field approximation the values obtained for the fit parameters were $M_0 \approx 14\,500$

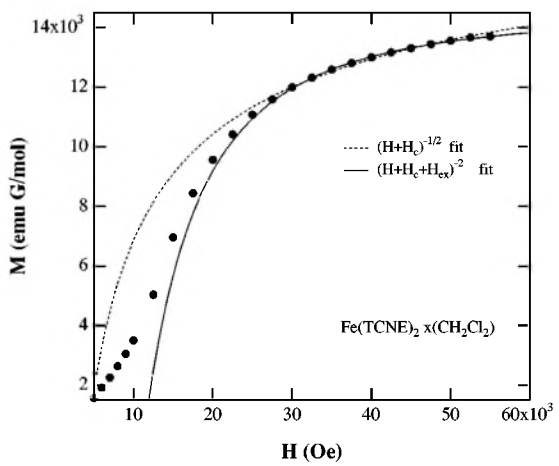

FIG. 12. $M(H)$ at 5 K (from the virgin hysteresis curve of Fig. 4) for dc fields up to 55 kOe. The dotted and the solid lines represent fits of $M(H)$ in the range $30 \leqslant H \leqslant 55$ kOe based on Eqs. (6) and (7), respectively.

emu Oe/mol, $H_r \approx 52.6$ kOe, and $H_c + H_{ex} \approx 2400$ Oe, the quality of the fit (measured as the sum of the deviations of the fit from the data squared) being ~ tenfold better than in the moderate field case.

The $(H+H_c+H_{ex})^{-2}$ dependence describes the $M(H)$ curve better than $(H+H_c)^{-1/2}$ and, therefore, the system should be either a RAM with small anisotropy (CSM) in a high field or a RAM with large anisotropy (SM) in a high field, but not a FWA. Moreover, we note that the maximum value of the exchange field ($H_{ex}=2.4$ kOe for $H_c \approx 0$) obtained from the large-field fit is much less than the applied fields used for the fit and, therefore, satisfies the condition of validity of the expression used [Eq. (7) is valid for $H_{ex} \ll H$].

To further distinguish between the two possibilities left we note the large value of the random anisotropy field compared to the exchange one, $H_r = 52.6$ kOe $\gg H_{ex} = 2.4$ kOe, which indicates a SM rather than a CSM. The only weakness of this result, raised by the condition of validity of Eq. (7) ($H_r < H$), is that the fit is strictly valid only at the higher extremity of the field range used.

Given the experimental evidence for RAM behavior mentioned above, the origins of randomenss need to be addressed, especially as $Fe(TCNE)_2 \cdot x(CH_2Cl_2)$ is partially crystalline. Although the concept of RAM was introduced to explain the anomalous magnetic behavior of amorphous systems it also has been applied in a crystalline context.[7] In the case of $Fe(TCNE)_2 \cdot x(CH_2Cl_2)$ the anisotropy is intrinsic to the Fe^{II} ion in a distorted octahedral environment. The randomness may be enhanced by dilution, likely caused by the solvent, just as was the case for $V(TCNE)_x \cdot y(solvent)$,[5,6,41] and increased by the various binding configurations of $[TCNE]^-$.[13,40]

The complex double-transition behavior of $Fe(TCNE)_2 \cdot x(CH_2Cl_2)$ is puzzling, as the crossover from CSM to SM is expected to lead to a zero spontaneous moment[20] not to an enhancement of it. Noting that the additional "freezing" and the increase of the remanent magnetization appear to occur simultaneously, we speculate that there may be a connection between ferrimagnetism and the enhancement of random anisotropy. Given the partial crystallinity of these compounds it is likely that a magnetic lattice exists at least locally within each crystallite and it consists of various sublattices, (made up of Fe^{2+}, and $[TCNE]^-$s, respectively) leading to ferrimagnetic configurations. The magnetic moment could increase upon decreasing the temperature due to the difference between the exchange couplings between the various sublattices and the different temperature variation of the sublattice moments, as was previously shown for ferrites[39] and $Mn(TCNE)_x \cdot y(CH_2Cl_2)$.[13] The various exchange interactions between sublattices may lead to low-T canted spin configurations,[47] which could increase the moment as the spins are no longer locally antiparallel. Favoring only particular (canted) spin configurations,[47] the exchange interactions also may contribute to an additional "stiffness" of the spins, resulting in a enhancement in anisotropy simultaneous with the increase in magnetic moment.

We end our discussion of $Fe(TCNE)_2 \cdot x(CH_2Cl_2)$ proposing that this system is an unusual candidate for a sperimagnet. While traditionally the term sperimagnet has been used for a system with rare-earth and transition-metal ions locally coupled antiferromagnetically but with random spin orientation due to the nonuniform anisotropy,[21,48] we suggest extension of this concept to a molecule-based magnet. Similar to the typical sperimagnet, in this case the spins located in the d orbitals and those located in the π^* organic orbitals interact antiferromagnetically, while the solvent dilution likely causes randomly distorted environments and, hence, RAM behavior.

VI. CONCLUSION

We reported extensive magnetic studies of $Fe(TCNE)_2 \cdot x(CH_2Cl_2)$, a high-$T_c$ molecule-based magnet with a mixture of ferrimagnetic and RAM charcateristics. The ferrimagnetic behavior is suggested by the constricted hysteresis curve with a spin-flop shape, the ac susceptibility in the presence of a dc field, consistent with the spin-flop picture, and the remanent magnetization suggest ferrimagnetic behavior. The spins on the Fe^{2+} ion and on the $[TCNE]^-$ ions likely form (at least locally) sublattices that couple antiferromagnetically.

The ac susceptibility data in zero dc field has weak frequency dependence (better seen in χ'', especially below ~20 K) suggesting glassiness while the FC/ZFC magnetization data shows irreversibilities, starting at ~97 K, and increasing below ~20 K, all consistent with double-transition RAM behavior. Ferromagneticlike scaling analysis reveals critical exponents relatively consistent with RAM predictions. Also, the curvature of the $T < T_c$ data in the modified Arrott plot is characteristic for RAM. The origin of randomness in this partially crystalline compound likely resides in the solvent vacancies and in the ability of $[TCNE]^-$ to bind in different orientations, both being able to change the environment around the transition-metal ion and hence the magnetic anisotropy.

A closer look at the $T < 20$ K behavior, where the glassy behavior is enhanced (suggesting a CSM to SM crossover upon decreasing T), and the remanent moment has a significant increase, leads us to speculate that the ferrimagnetic and RAM behaviors might be correlated. We proposed that the various exchange interactions between local sublattices may

lead to low-T canted spin configurations, which could increase the local moment as the spins are no longer (locally) antiparallel. Simultaneously, increased anisotropy may occur due to the additional ''stiffness'' induced by the exchange interactions favoring only specific spin configurations. Based on this complex behavior we proposed that $Fe(TCNE)_2 \cdot x(CH_2Cl_2)$ is a molecule-based candidate for a sperimagnet, evolving from a correlated sperimagnet below 97 K to a sperimagnet below 20 K.

ACKNOWLEDGMENTS

We acknowledge the financial support provided by the U.S. DOE under Grants No. DE-FG02-86ER45721, DE-FG03-93ER45504, and DE-FG02-96ER12198.

*Present address: Department of Physics, Ovidius University of Constanţa, Constatnta 8700, Romania.
†Present address: XonTech, Inc., Van Nuys, CA 91406.
‡Present address: Akashic Memories Corporation, Santa Clara, CA 95054.

[1] J.M. Manriquez, G.T. Yee, R.S. Mclean, A.J. Epstein, and J.S. Miller, Science **252**, 1415 (1991).
[2] Proceedings of the 4th International Conference on Molecule-Based Magnets, edited by J.S. Miller and A.J. Epstein [Mol. Cryst. Liq. Cryst. Sci. Technol., Sect. A **271/274** (1995)]; Proceedings of the 5th International Conference on Molecule-Based Magnets, edited by K. Itoh, T. Takui, and J.S. Miller [*ibid.* **305/306** (1997)]; O. Khan, *Molecular Magnetism* (VCH, New York, 1993); J.S. Miller and A.J. Epstein, Angew. Chem. Int. Ed. Engl. **33**, 385 (1994).
[3] J.S. Miller and A.J. Epstein, J. Chem. Soc. Chem. Commun. **1998**, 1319.
[4] J.S. Miller and A.J. Epstein, Chem. Industry **15**, 49 (1996); J.S. Miller and A.J. Epstein, Chem. Eng. News **73**, 30 (1995).
[5] P. Zhou, B. G. Morin, J. S. Miller, and A. J. Epstein, Phys. Rev. B **48**, 1325 (1993).
[6] P. Zhou, S.M. Long, J.S. Miller, and A.J. Epstein, Phys. Lett. A **181**, 71 (1993).
[7] P.M. Gehring, M.B. Salamon, A. del Moral, and J.I. Arnaudas, Phys. Rev. B **41**, 9134 (1990).
[8] J. Filippi, V.S. Amaral, and B. Barbara, Phys. Rev. B **44**, 2842 (1991).
[9] M. J. O'Shea, K.M. Lee, and A. Fert, J. Appl. Phys. **67**, 5769 (1990).
[10] D.J. Sellmyer and M.J. O'Shea, in *Recent Progress in Random Magnets*, edited by D.H. Ryan (World Scientific, Singapore, 1992).
[11] Y.Y. Goldschmidt, in *Recent Progress in Random Magnets* (Ref. 10).
[12] J. Zhang, J. Ensling, V. Ksenofontov, P. Gutlich, A.J. Epstein, and J.S. Miller, Angew. Chem. Int. Ed. Engl. **37**, 657 (1998); J. Zhang, L.M. Liable-Sands, A.L. Rheingold, R.E. Del Sesto, D.G. Gordon, B.M. Burkhart, and J.S. Miller, J. Chem. Soc. Chem. Commun. **1998**, 1385.
[13] C.M. Wynn, M.A. Gîrţu, J. Zhang, J.S. Miller, and A.J. Epstein, Phys. Rev. B **58**, 8508 (1998).
[14] S.F. Edwards and P.W. Anderson, J. Phys. (France) **5**, 965 (1975); D. Sherington and S. Kirkpatrick, Phys. Rev. Lett. **35**, 1792 (1975).
[15] D.S. Fisher and D.A. Huse, Phys. Rev. B **38**, 386 (1988).
[16] R. Harris, M. Plischke, and M.J. Zuckermann, Phys. Rev. Lett. **31**, 160 (1973).
[17] R.W. Cochrane, R. Harris, and M.J. Zuckermann, Phys. Rep. **48**, 1 (1978).
[18] A. Aharony and E. Pytte, Phys. Rev. Lett. **45**, 1583 (1980).
[19] Y.Y. Goldschmidt and A. Aharony, Phys. Rev. B **32**, 264 (1985).
[20] E.M. Chudnovsky, W.M. Saslow, and R.A. Serota, Phys. Rev. B **33**, 251 (1986).
[21] J.M.D. Coey, J. Appl. Phys. **49**, 1646 (1978).
[22] Y. Imry and S.K. Ma, Phys. Rev. Lett. **35**, 1399 (1975).
[23] P.M. Chaikin and T.C. Lubensky, *Principles of Condensed Matter Physics* (Cambridge University Press, Cambridge, 1995).
[24] S.N. Kaul, J. Magn. Magn. Mater. **53**, 5 (1985).
[25] A. Arrott and J.E. Noakes, Phys. Rev. Lett. **19**, 786 (1967).
[26] A. Arrott, Phys. Rev. **108**, 1394 (1957).
[27] D.J. Sellmyer and S. Nafis, J. Appl. Phys. **57**, 3584 (1985).
[28] B. Dieny and B. Barbara, J. Phys. (France) **46**, 293 (1985).
[29] J.A. Mydosh, *Spin Glasses: An Experimental Introduction* (Taylor and Francis, London, 1993).
[30] K. Binder and A.P. Young, Rev. Mod. Phys. **58**, 801 (1986).
[31] B. Barbara, B. Dieny, and J. Fillipi, J. Appl. Phys. **67**, 5763 (1990).
[32] A. Abragam and B. Bleaney, *Electron Paramagnetic Resonance of Transition Ions* (Dover, New York, 1986).
[33] R.L. Carlin, *Magnetochemistry* (Springer-Verlag, Belin, 1986).
[34] Anomalies between the observed and the expected molar susceptibility and Curie constants also were observed in the $V(TCNE)_x \cdot y$ (solvent), see A.J. Epstein and J.S. Miller, Mol. Cryst. Liq. Cryst. Sci. Technol., Sect. A **228**, 99 (1993), and in $Mn(TCNE)_2 \cdot x(CH_2Cl_2)$ (Ref. 13).
[35] E. Strayjewski and N. Giordano, Adv. Phys. **28**, 487 (1977).
[36] R. Reisser, M. Seeger, and H. Kronmuller, J. Magn. Magn. Mater. **128**, 321 (1993).
[37] P.D. Babu and S.N. Kaul, Phys. Rev. B **52**, 10 637 (1995).
[38] C.M. Wynn, M.A. Gîrţu, J.S. Miller, and A.J. Epstein, Phys. Rev. B **56**, 315 (1997); **56**, 14 050 (1997); C.M. Wynn, M.A. Gîrţu, W.B. Brinckerhoff, K-I. Sugiura, J.S. Miller, and A.J. Epstein, Chem. Mater. **9**, 2156 (1997).
[39] E.W. Gorter, Philips Res. Rep. **9**, 295 (1954); **9**, 321 (1954); **9**, 403 (1954).
[40] M.A. Gîrţu, C.M. Wynn, K.I. Sugiura, J.S. Miller, and A.J. Epstein, J. Appl. Phys. **81**, 4410 (1997); Synth. Met. **85**, 1703 (1997).
[41] B.G. Morin, P. Zhou, C. Hahm, and A.J. Epstein, J. Appl. Phys. **73**, 5648 (1993).
[42] K.M. Lee and M.J. O'Shea, J. Appl. Phys. **67**, 5781 (1990).
[43] T. Kaneyoshi, *Amorphous Magnetism* (CRC, Boca Raton, 1984).
[44] W.B. Brinckerhoff, Jie Zhang, J.S. Miller, and A.J. Epstein, Mol. Cryst. Liq. Cryst. Sci. Technol., Sect. A **272**, 195 (1995).
[45] M.J. O'Shea and K.M. Lee, J. Magn. Magn. Mater. **99**, 103 (1991).
[46] M.J. O'Shea, K.M. Lee, and F. Othman, Phys. Rev. B **34**, 4944 (1986).
[47] Y. Yafet and C. Kittel, Phys. Rev. **87**, 290 (1952).
[48] C.M. Hurd, Contemp. Phys. **23**, 469 (1982).